Journal of Power Sources 390 (2018) 1–12

Contents lists available at ScienceDirect

Journal of Power Sources

journal homepage: www.elsevier.com/locate/jpowsour

Highly conducting blend hybrid electrolytes based on amine ended block copolymers and organosilane with in-situ formed silica particles for lithium-ion batteries

Diganta Saikia[a], Yu-Ju Chang[a], Jason Fang[b], Hsien-Ming Kao[a,*]

[a] Department of Chemistry, National Central University, Chung-Li, 32054, Taiwan, ROC
[b] Department of Fuel Cell Materials and Advanced Capacitors, Division of Energy Storage Materials and Technology, Material and Chemical Laboratories, Industrial Technology Research Institute, Hsin-Chu 300, Taiwan, ROC

HIGHLIGHTS

- Solid and plasticized electrolytes are synthesized from the same blend hybrid matrix.
- The hybrid SPE exhibits maximum ionic conductivity of 1.1×10^{-4} S cm^{-1} at 30 °C.
- The PPE membrane reveals an extremely high conductivity of 24 mS cm^{-1} at 30 °C.
- The cell delivers initial capacity of 142 mAh g^{-1} with 92% retention after 70 cycles.

GRAPHICAL ABSTRACT

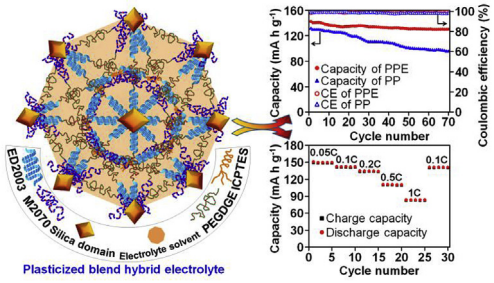

ARTICLE INFO

Keywords:
Hybrid electrolyte
Blend
Ionic conductivity
Electrochemical stability window
Lithium-ion battery

ABSTRACT

In this study, amine ended block co-polymers of ethylene oxide/propylene oxide units are reacted separately with poly(ethylene glycol) diglycidyl ether (PEGDGE) and (3-isocyanatopropyl)triethoxysilane (ICPTES) and then mixed in different weight ratios to obtain ion conductive and mechanically stable hybrid solid polymer electrolytes (SPEs). Various characterization techniques are employed to explore the morphology, thermal stability, molecular interaction, backbone structure and dynamic behavior of the blend hybrid SPEs. The hybrid SPE exhibits the maximum ionic conductivity of 1.1×10^{-4} S cm^{-1} at 30 °C. The electrochemical stability window of hybrid SPEs varies from 4.5 to 4.7 V, depending on salt concentration. Moreover, the "salt free" hybrid membrane is plasticized in an organic electrolyte solvent to enhance the ionic conductivity to an exceptionally high value of 2.4×10^{-2} S cm^{-1} at 30 °C and 1.8×10^{-1} S cm^{-1} at 70 °C. The test cell consists of plasticized blend hybrid membrane delivers an initial discharge capacity of 142.5 mAh g^{-1} and retains 92% of initial capacity after 70 cycles with coulombic efficiency value of over 99%. Our results show that the blend hybrid electrolytes can be a promising electrolyte system for applications in high energy density lithium-ion batteries.

1. Introduction

The technological prowess and environmental concerns have prompted researchers to develop devices to use renewable energy resources and/or effectively store them. Among storage devices, lithium-ion battery (LIB) is the most promising and increasingly demandable battery system due to its high energy density in comparison to other battery technologies, which finds applications from consumer

* Corresponding author.
E-mail address: hmkao@cc.ncu.edu.tw (H.-M. Kao).

https://doi.org/10.1016/j.jpowsour.2018.04.028
Received 7 September 2017; Received in revised form 8 March 2018; Accepted 7 April 2018
Available online 24 April 2018
0378-7753/

electronic products to hybrid electric vehicles/electric vehicles (HEVs/EVs) [1,2]. However, with the continuous technological advancement in the consumer products, the development of more powerful batteries is utmost important. Electrolyte is one of the key components of battery that needs urgent attention to fulfil the goal of developing high power batteries. However, development of an efficient and high performance electrolyte for next generation lithium-ion batteries is still a challenge. The classical lithium-ion batteries presently available in the market mostly use lithium salts to be dissolved in organic solvents as electrolytes in order to offer ionic conductivity values on the order of 10^{-3} S cm^{-1} or higher. Still, high flammability of organic solvents, formation of lithium dendrite, thermal instability and solvents leakage have raised serious concerns on safety and overall performance of LIBs [3,4]. Solid polymer electrolytes (SPEs) are considered as effective alternatives to liquid electrolytes to overcome the drawbacks mentioned above [5–7]. SPEs have their advantages such as good flexibility, facile processability, low interfacial resistance and good interfacial contacts with electrodes. Since the pioneering works carried out by Wright and Armand groups on poly(ethylene oxide) (PEO) based SPEs, much research effort has focused on SPEs for acknowledging their potentials in rechargeable batteries [8,9]. However, poor ionic conductivity of PEO-based SPEs at room temperature, mostly from 10^{-7} to 10^{-5} S cm^{-1} seriously impedes their applications in LIBs.

In an effort to address the issue of low ionic conductivity of PEO-based SPEs, several alternative strategies, such as semi-interpenetrating network polymer electrolytes, blend polymer electrolytes, branched polymer electrolytes, composite polymer electrolytes, block co-polymer electrolytes and salts dissolved in different types of polymeric matrices have been tested out and achieved mixed results in boosting ionic conductivity [10–16]. In addition, some of these electrolytes also entangle with deficiencies, for example, particle aggregation in composite SPEs, inferior mechanical strength and narrow electrochemical stability window that prohibits their practical use in LIBs. Poor mechanical properties of SPEs additionally raise safety concerns, due to the short circuit between the electrodes in the batteries at elevated temperature. Therefore, here is a great scope to explore new SPEs that can overcome these drawbacks. In search of high performance electrolytes, organic-inorganic hybrid electrolytes have gained considerable interests because of their higher ionic conductivity at room temperature [17–19]. Moreover, these organic-inorganic hybrids can improve the interfacial contact between electrolyte and electrodes due to their flexible design and adhesiveness. These hybrid SPEs can possess unique physical and chemical properties by changing the amount of organic and inorganic components according to requirements. Furthermore, the functionalization level can be easily controlled as the sol-gel process mainly involved in the synthesis of these hybrids. Therefore, the hybrid electrolytes could synergistically combine the beneficial properties of both organic and inorganic components to form a mechanically stable free-standing membrane. Another important fact is that these hybrid SPEs can be easily converted to plasticized polymer electrolytes (PPEs) by simply swelling the membranes in organic solvents without deterioration of mechanical properties. PPEs are safer than liquid electrolytes because they can uptake solvent efficiently and retain it inside the pores of the polymeric matrix without leakage, and thus prevent any fire or explosion hazards at the time of battery malfunction. Normally, the ionic conductivity of PPEs is in the ranges of 10^{-3} to 10^{-2} S cm^{-1} and suitable for good charge-discharge and life cycle performance of battery systems [20–22]. In addition, well compatibility with the electrodes and wide electrochemical windows make PPEs the electrolyte of choice [20–22].

In the present work, we devote our effort to blend two polymer precursors with different chain lengths to make SPEs with in-situ formed silica particles to give the composite nature. Then the same blend hybrid membrane is employed to make PPEs that are further used as separators in lithium-ion batteries to evaluate the electrochemical performances. Blending eases the synthesis procedure of the hybrid electrolytes while maintaining higher ionic conductivity as well as thermal and mechanical integrity. The blend hybrid electrolytes can be composed of the soft and hard components from two polymer precursors with the soft part mainly responsible for ionic conduction, while the hard part for thermal and mechanical strength [11,13]. Based on the above strategies, herein we reports a new type of blend organic-inorganic hybrid electrolyte that is formed by blending two different polymer precursors: one is formed by polymerization of polyetheramine (M-2070) and poly(ethylene glycol) diglycidyl ether (PEGDGE) (precursor I), and the other is from the reaction of polyetherdiamine (ED2003), PEGDGE and (3-isocyanatopropyl)triethoxysilane (ICPTES) (precursor II). The N=C=O functional group in the organosilane ICPTES is highly reactive towards the NH_2 end groups of polyetherdiamine (ED2003), and thus allows these functional groups to bond covalently to make the stable hybrid structure. Further, it generates in-situ sub-micron sized silica particles after hydrolysis and condensation reactions, which have positive effects in improving the electrical and mechanical properties of the electrolyte. The blending amount of precursors and salt concentrations are varied and optimized to prepare the blend hybrid SPEs. The physical and chemical behaviors of the blend hybrid SPEs are characterized by DSC/TGA, wide angle XRD and FTIR analysis. The structural integrity and dynamic properties of the blend hybrid SPEs are analyzed with multinuclear (^{13}C, ^{29}Si, and ^{7}Li) solid-state NMR spectroscopy. The electrochemical characterizations, such as AC impedance and linear sweep voltammetry (LSV) are determined to obtain the ionic conductivity and electrochemical stability window of the blend hybrid SPEs. For testing the battery performance of the blend hybrid system, the pristine blend hybrid membrane (without salt) is swelled in different electrolyte solvents and its ionic conductivity and LSV are measured. To the end, the lithium-ion battery is assembled with the blend hybrid PPE using lithium metal and $LiFePO_4$ electrodes and its cycle performance and capacity at different current rates are measured.

2. Experimental section

2.1. Synthesis of blend hybrid SPEs

For the preparation of the blend hybrid SPEs, two polymer precursors were synthesized in the first place. The synthesis procedure is schematically described in Fig. 1. In the first phase, 2 mol of polyetheramine M-2070 (Jeffamine M-2070 with M_w = 2000 g mol^{-1}, Huntsman) and 1 mol of PEGDGE (M_w = 526 g mol^{-1}, Aldrich) were dissolved in 15 mL of tetrahydrofuran (THF) separately and then mixed together and stirred at 50 °C for 24 h to complete the reaction to form the precursor I. In the second phase, 2 mol of polyetherdiamine (Jeffamine ED2003, M_w = 2000 g mol^{-1}, Huntsman) and 1 mol of PEGDGE were dissolved in 15 mL of THF separately and then mixed both the solutions and stirred at 50 °C for 24 h to complete the reaction. Afterwards, 2 mol of ICPTES (Aldrich) was added to the reaction mixture and stirred at 60 °C for 24 h to attach the silane chains to the polymeric matrix. Subsequently, a small amount of 1 M HCl (0.3 mL) was added to the mixed solution to facilitate the hydrolysis and condensation reactions of ICPTES in order to form the silica network architecture within the polymeric matrix. The resulting product was denoted as the precursor II. The hydrolysis and condensation reactions of the organosilanes took place as follows:

$$\equiv Si - OR + H_2O \xrightarrow{Hydrolysis} \equiv Si - OH + ROH \quad (1)$$

$$\equiv Si - OH + \equiv Si - OH \xrightarrow{Water\ condensation} \equiv Si - O - Si \equiv + H_2O \quad (2)$$

Silanol groups are generated from the hydrolysis of ICPTES. Condensation of these silanol groups forms the siloxane bridges (Si–O–Si) that build the whole silica structure and finally forms the in-

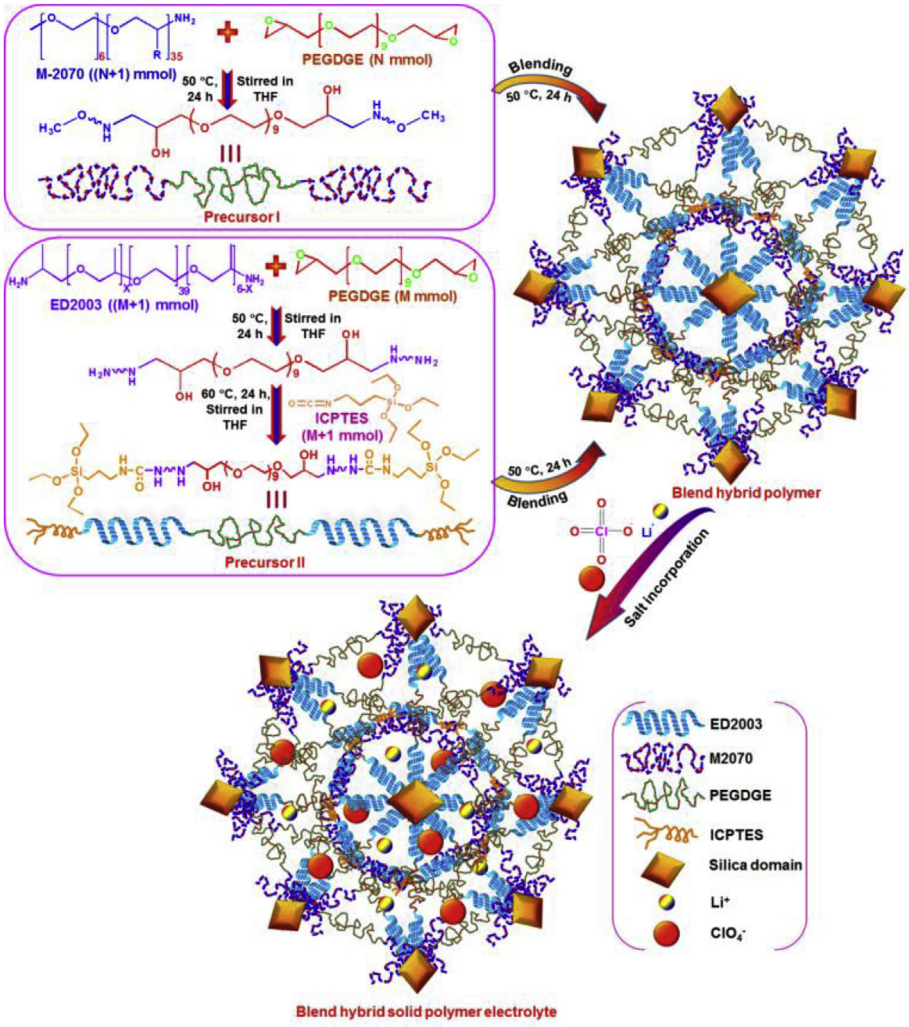

Fig. 1. Schematic representation of the synthesis of blend hybrid electrolyte membrane.

situ sub-micron sized silica particles. The N = C = O functionality at the other end of ICPTES reacts with the NH_2 end groups of ED2003 and covalently bonded to form the hybrid structure as shown in Fig. 1. As these silica particles are attached to the polymeric units, they are expected to be dispersed uniformly in the hybrid structure, and thus any agglomeration of these particles can be effectively reduced. To make the blend hybrid SPEs, these two precursors were mixed in different weight ratios, stirred for 24 h at 50 °C. Then, the desired [O]/[Li] ratio was achieved by adding appropriate amounts of the lithium salt $LiClO_4$ into the mixture solution. After further stirred for 24 h, the final viscous solution was cast onto Teflon dishes and vacuum dried at 70 °C to obtain the blend hybrid SPEs with thickness ranging from 80 to 90 μm. The relative amounts of precursors I and II in the blend hybrid SPEs were varied and optimized to ensure that the blend hybrid SPEs possessed enough mechanical strength and good elasticity. The blend hybrid SPEs are designated as PD(x:y)-Z, where P represents the precursor I (composed of PEGDGE and M-2070), D corresponds to the precursor II (composed of ED2003, PEGDGE, and ICPTES), x and y indicate the weight percentages of precursors I and II, respectively, that are used to make the blend hybrid SPEs, and Z relates to the [O]/[Li] ratio calculated by considering the ether oxygens (exclusively from M-2070, ED2003 and PEGDGE) per Li^+ cations.

2.2. Synthesis of blend hybrid PPEs

Since the ionic conductivity of the blend hybrid SPEs is not high enough at room temperature, it is difficult to obtain a good charge-discharge and cycle performance from a LIB based on the blend hybrid SPEs thus obtained, which have an ionic conductivity value lower than 10^{-3} S cm^{-1} at room temperature. Based on the optimal ratio of precursor I and precursor II, the blend hybrid PPEs were prepared instead with the same architecture of SPEs by following the procedure mentioned above, but without the addition of lithium salt. The "salt free" blend hybrid membrane was swelled in organic electrolyte solvents of 1 M LiTFSI in EC/PC (1:1, v/v), 1 M $LiPF_6$ in EC/DEC (1:1, v/v), and 1 M LiOTf in EC/PC (1:1, v/v) in order to obtain the blend hybrid PPEs for further lithium-ion battery applications.

2.3. Fabrication of lithium-ion battery

The blend hybrid PPE membrane with the optimal properties was used to fabricate the lithium-ion battery and to test its performance. The fabrication process was carried out under argon atmosphere with less than 1 ppm oxygen that was provided by a glove box (PL-HE-2GB with PL-HE-GP1 inert gas purifier, Innovative technology). Lithium metal (Sigma-Aldrich) was used as anode. A slurry consisting of 80 wt% $LiFePO_4$, 10 wt% super P carbon and 10 wt% PVdF binder in a NMP (*N*-methyl-2-pyrrolidone) solution was used to make the cathode. The slurry was then blade coated on aluminum foil and dried overnight at 100 °C. Afterwards, the dried coated foil was roller-pressed and punched to make the circular cathode disc of appropriate size for the 2032 coin cell. The blend hybrid membrane was dipped in 1 M $LiPF_6$ in EC/

DEC (1:1, v/v) for 30 min to uptake the electrolyte solvent and then sandwiched between lithium anode and $LiFePO_4$ cathode to assemble the battery.

2.4. Characterization methods

Differential scanning calorimetry (DSC, Perkin-Elmer Pyris 6) and thermogravimetric analysis (TGA, TA instruments Q50) were performed on the blend hybrid SPEs with a heating rate of 10 °C min^{-1} under nitrogen environment. Wide-angle X-ray diffraction (WXRD) of the SPE samples were recorded in Shimadzu diffractometer (Lab-X XRD 6000) with a monochromatic Cu K_α radiation ($\lambda = 0.15406$ nm). Fourier transform infrared (FTIR) spectroscopy was carried out in a JASCO 4200 spectrometer in the frequency range of 4000–500 cm^{-1} at a resolution of 4 cm^{-1}. To investigate the salt interaction with the polymer, the FTIR spectra were further deconvoluted in the frequency region of 660–600 cm^{-1}. Mechanical strength of the blend hybrid electrolytes membranes was measured in a TA instruments' Q800 dynamic mechanical analyzer (DMA). Tests were conducted with the application of 0.5 N min^{-1} force to the samples. Nova NanoSEM 230 (FEI) scanning electron microscope (SEM) was used to study the morphology of the blend hybrid electrolyte membranes.

^{13}C, ^{29}Si and ^{7}Li solid-state NMR measurements were carried out on Varian Infinityplus-500 NMR spectrometer with the Larmor frequencies of 125.36, 99.03 and 194.3 MHz for ^{13}C, ^{29}Si and ^{7}Li spins, respectively. The Hartmann-Hahn matching conditions of cross-polarization magic angle spinning (CPMAS) for ^{13}C and ^{29}Si spins were established by using admantane and octakis(trimethylsiloxy)-silsesquioxane (Q_8M_8) as standards, respectively. The chemical shifts were referred to tetramethylsilane (TMS) at 0 ppm for ^{13}C and ^{29}Si nuclei while 1 M $LiCl_{(aq)}$ at 0 ppm was used as reference for ^{7}Li. With the use of 2D WISE (two-dimensional WIdeline SEparation spectroscopy) NMR pulse sequence, the ^{1}H wide line spectra were obtained from the proton of the polymer chains along the ω_1 dimension, which were resolved by the ^{13}C chemical shifts of the polymer chains along the ω_2 dimension.

AC impedances of the blend hybrid SPEs and PPEs were conducted on an Autolab/PGSTAT302 (Metrohm Autolab B.V., Netherlands) frequency response analyzer and measured within the selected frequency range of 100 kHz to 1 Hz with amplitude of 10 mV. The impedance data were collected from 10 to 70 °C. Each sample was equilibrated thermally at the measured temperature for at least 30 min before recording the data. Based on the impedance data, the ionic conductivity (σ) of the blend hybrid electrolytes was measured by the equation $\sigma = (1/R_b)(t/A)$; where R_b corresponds to the bulk electrolyte resistance, t represents the thickness of the membrane, and A the area of the electrode. The R_b values can be determined from the intercept of the real axis of the complex impedance plot.

The LSV technique, measured from 0 to 6 V vs. Li/Li^+ at a scan rate of 1 mV s^{-1}, was used to explore the electrochemical stability window of the blend hybrid electrolytes by assembling a coin-cell with stainless steel (SS) as working electrode and lithium as counter and reference electrode and sandwiching the sample in-between them.

A battery testing system (LANHE CT2001A) was employed to evaluate the cell performances, such as charge-discharge behaviors and cycle life, at a current rate of 0.1C. The charge-discharge performances were also measured with varying current rates to assess the stability of the cell under different current values.

3. Results and discussion

3.1. Evaluation of the blending percentage of hybrid SPEs by ionic conductivity measurements

It is crucial to optimize the blending ratio in a blend hybrid electrolyte in the first place in order to design a suitable electrolyte with good flexibility, mechanical strength, and electrochemical stability as well as high ionic conductivity. Therefore, the present PD(x:y)-Z SPEs are evaluated by varying the weight percentages of the precursors I and II, while keeping a [O]/[Li] ratio of 32. The relative amounts of two precursors are varied from x:y = 30:70 to x:y = 70:30 for the precursors I and II. The temperature dependence of ionic conductivity for PD(x:y)-32 as a function of the weight ratios (x:y) of two precursors is depicted in Fig. S1 (Supplementary Information, SI). It is found that the PD(70:30)-32 blend hybrid electrolyte exhibits the maximum ionic conductivity of 1.7×10^{-4} S cm^{-1} at 30 °C. The conductivity has started to decrease with the reduction in the amount of the precursor I and the increment in the amount of the precursor II with values varying from 1.1×10^{-4} S cm^{-1} for PD(60:40)-32 to 3.9×10^{-5} S cm^{-1} for the PD(30:70)-32 samples at 30 °C. Although the PD(70:30)-32 sample exhibits the maximum ionic conductivity, it is not mechanically strong enough to be used as separator in lithium-ion batteries. The amount of the soft component (precursor I) is higher in the PD(70:30)-32 sample (70%) than the PD(60:40)-32 sample (60%), which makes the former mechanically poorer. The stress-strain curve of the PD(70:30)-32 SPE membrane is depicted in Fig. S2 (SI). It is observed that PD(70:30)-32 blend hybrid SPE membrane possesses not sufficient mechanical strength to be used as separator in LIBs. As the electrolyte membrane is not mechanically stable, it may lose interfacial contacts and can cause short circuit, thus hinder the long cycle life of battery. Therefore, it is necessary to maintain proper mechanical strength as well as ionic conductivity by a good electrolyte membrane. Instead, the PD(60:40)-Z system, which is mechanically strong and flexible, is chosen as an alternative for further characterization with varying [O]/[Li] ratios to study the effects of lithium-ion concentrations.

3.2. X-ray diffraction analysis of the blend hybrid SPEs

Wide-angle X-ray diffraction (WXRD) measurements are carried out to analyze the changes in the crystallinity behavior of the blend hybrid SPEs with different salt concentrations. The XRD patterns of $LiClO_4$ salt, pristine ED2003 and the blend hybrid SPEs with various salt concentrations are depicted in Fig. 2A. The lithium salt $LiClO_4$ shows intense peaks at 2θ values of 21.3, 23.3, 31.7, 33.1, 35.8 and 39.6°, identifying its crystalline nature (Fig. 2A(a)). The pristine ED2003 also exhibits two sharp peaks at 2θ values of 19.4 and 23.5°, indicative of the crystalline structure of the polymer ED2003 (Fig. 2A(b)). However, existence of some small broad peaks implies partial amorphous nature of ED2003. This semi-crystalline morphology of ED2003 changes to almost amorphous structure with the formation of blend hybrid SPEs by introduction of lithium salt (Fig. 2A(c-g)). The complete dissolution of the salt in the blend hybrid SPEs is confirmed by the absence of the $LiClO_4$ peaks. It is also observed that the crystallinity gradually decreases with the increase in the salt concentration as reveal by the enhancement in broadening of the peaks. It suggests that the increased interaction of the salt with the polymer breaks some regular bonds in the polymer network leading to an increase in the amorphous phase in the electrolyte sample. This can be beneficial for the blend hybrid SPEs as it is widely believed that the amorphous phase plays a crucial role in the ionic movements and thus influences the ionic conductivity.

3.3. Thermal properties of the blend hybrid SPEs

DSC is a thermoanalytical technique which can be utilized to acquire information on glass transition temperature (T_g), degree of crystallinity (χ_c) and complexation behavior of the salt with the polymeric matrix. Fig. 2B displays the DSC thermograms of the pure polymers and the blend hybrid SPEs with various salt concentrations. As shown in Fig. 2B, the thermogram of pure ED2003 shows a melting transition at 35.4 °C, while M-2070 presents a melting transition around 0.1 °C. In the case of blend hybrid SPEs, the melting peak appears at 18.7 °C for the PD(60:40)-48 sample and continuously shifts toward lower temperatures with increase in the salt concentrations, and finally reaches

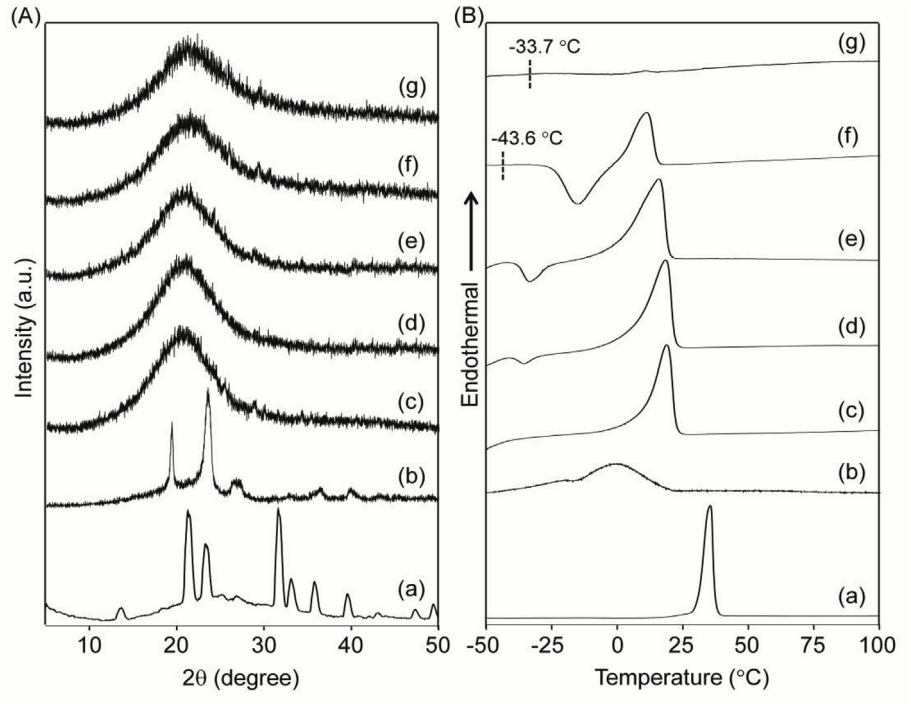

Fig. 2. (A) WXRD patterns of (a) $LiClO_4$, (b) ED2003 and PD(60:40)-Z blend hybrid SPEs with Z = (c) 48, (d) 40, (e) 32, (f) 24 and (g) 16. (B) DSC thermograms of (a) ED2003, (b) M-2070, and PD(60:40)-Z blend hybrid SPEs with Z = (c) 48, (d) 40, (e) 32, (f) 24 and (g) 16.

11.3 °C for the PD(60:40)-24 SPE sample. The blend hybrid SPEs show almost no melting transition when the [O]/[Li] ratio is 16 or higher. As the melting transition is directly related to the degree of crystallinity, it is clear from the observed changes that the crystalline phase is converted to the amorphous phase with the increase in salt concentrations. Thus, incorporation of salt suppresses the degree of crystallinity. It is possible to estimate the degree of crystallinity (χ_c) from the area under the melting peak by following the equation

$$\chi_c = \frac{\Delta H_{SPE}}{\Delta H_{ED2003}} \times 100\% \quad (3)$$

where ΔH_{ED2003} and ΔH_{SPE} are the enthalpies of fusion of the pure ED2003 and the blend hybrid SPEs, respectively. Considering the pure ED2003 as 100% crystalline, the degree of crystallinity of the blend hybrid SPEs with various salt concentrations are calculated, and the results are listed in Table 1 along with the enthalpy values. The data from Table 1 clearly shows that with increase in the salt concentrations the endothermic heat decreases, resulting in a decrease in the relative crystallinity. The PD(60:40)-48 sample with a lower salt concentration possesses 47.5% relative crystallinity as compared to just 2% for the PD (60:40)-16 sample with a higher salt concentration, suggesting the conversion from semi-crystalline phase to almost amorphous phase. It is believed that the increased interactions of oxygen atoms from polyether units of polymers and Li^+ cations from $LiClO_4$ salt prohibit the reorganization of the polymer chains or break the regular crystallized structure which in turn reduces the degree of crystallinity [23]. For the blend hybrid SPEs with medium salt concentrations (i.e., [O]/[Li] = 40–24), an exothermic peak around −35.4 °C is observed for the PD(60:40)-40 sample, which is shifted to −14.8 °C for PD(60:40)-24 SPE and completely disappears at a higher salt concentration of [O]/[Li] = 16. The recrystallization of some polyether based polymeric units may generate such exothermic peaks in the medium salt concentrations, while this phenomenon is completely suppressed by a higher salt content, e.g., the PD(60:40)-16 SPE sample [24].

Table 1
Glass transition temperature (T_g), melting temperature (T_m), enthalpy of fusion (ΔH), degree of crystallinity (χ_c) and number of free ions of the PD(60:40)-Z blend hybrid SPEs.

Sample	T_g (°C)	T_m (°C)	ΔH (J g^{-1})	χ_c (%)	Number of free ions
ED2003	–	35.4	96.3	100	–
M-2070	–	0.1	21.9	22.7	–
PD(60:40)-48	–	18.8	45.8	47.5	2.3×10^{20}
PD(60:40)-40	–	18.6	41.2	42.7	2.7×10^{20}
PD(60:40)-32	–	15.8	37.2	38.6	3.0×10^{20}
PD(60:40)-24	–43.6	11.3	21.9	22.7	3.9×10^{20}
PD(60:40)-16	–33.7	10.8	2.1	2.1	4.6×10^{20}

The T_g value is an important parameter that allows one to distinguish at what temperature the blend hybrid SPE is soft and rubbery or hard and brittle. Fig. 2B shows the T_g values for blend hybrid SPEs with the [O]/[Li] ratios of 24 and 16. The measurements of the T_g values for other samples are not possible due to the limitation of our instrument in cooling below −50 °C. Nevertheless, there is no transition observed above −50 °C for the blend hybrid SPEs with the [O]/[Li] ratios from 48 to 32, confirming that their T_g values are all below −50 °C. The PD (60:40)-24 sample exhibits a T_g value of −43.6 °C, which is lower than PD(60:40)-16 sample with a higher salt concentration (T_g = −33.7 °C). Therefore, it suggests that increase in the salt concentration effectively enhances the interaction of oxygen atoms in polyether units with the Li^+ cations, leading to a gradual increase in the T_g values and polymer chain stiffness [25]. The thermal stability of the blend hybrid SPEs is measured by TGA, and the results are displayed in Fig. S3 (SI). It is observed that the PD(60:40)-Z blend hybrid SPEs are thermally stable up to 240 °C without any degradation, which may be suitable for applications in electrochemical devices at high temperatures. The detailed weight loss steps are described in the SI.

3.4. Structural information and ion-transport analysis from FTIR

The FTIR spectra of the blend hybrid SPEs with various salt concentrations and without addition of salt are depicted in Fig. 3. The characteristic bands for N–H stretching mode (3460 cm^{-1}), symmetric

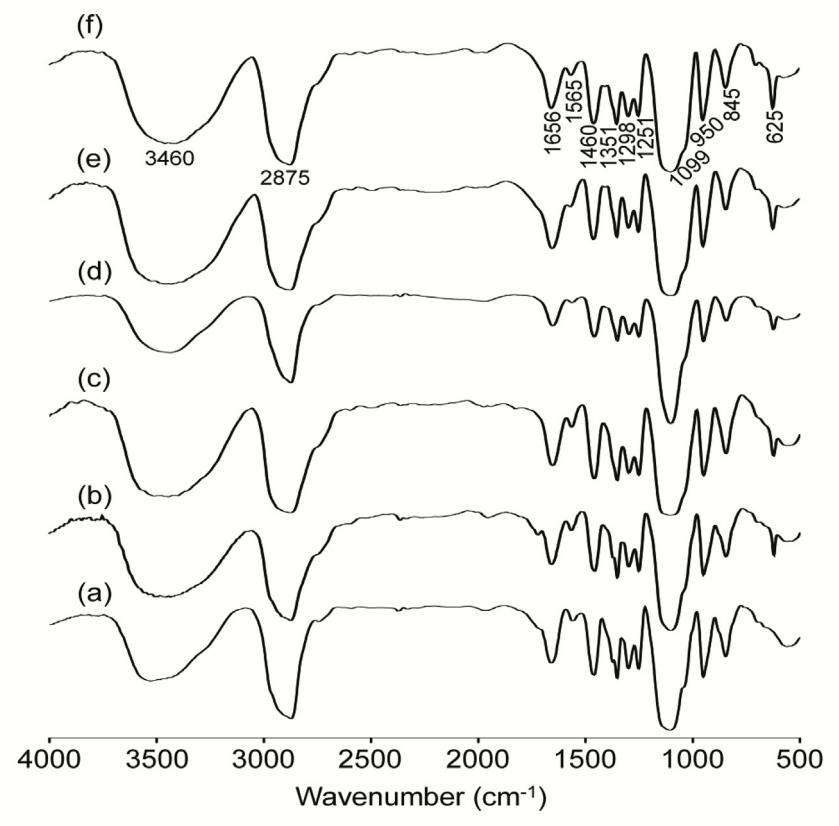

Fig. 3. FTIR spectra of PD(60:40)-Z blend hybrid SPEs with Z = (a) ∞, (b) 48, (c) 40, (d) 32, (e) 24 and (f) 16.

$-CH_2$ stretching (2875 cm^{-1}), N–H bending (1565 cm^{-1}), C–N stretching (1656 and 1298 cm^{-1}), $-CH_2$ vibrational modes, such as bending (1460 cm^{-1}), wagging (1351 cm^{-1}), twisting (1251 cm^{-1}), rocking (845 cm^{-1}) and C–O–C stretching (1099 cm^{-1}) are observed for all the samples [26–31]. As the hydrolysis of ICPTES gives rise to the Si–O–C and Si–O–Si linkages, the vibrational bands related to these units should be observed around 1050 to 1150 cm^{-1} [30,32]. However, due to overlapping of these bands with C–O–C vibration, it is not possible to specify these interactions separately. It is possible that silicon may not condense completely in the hydrolysis and condensation reactions of ICPTES and generates a band for non-condensed Si–OH at 950 cm^{-1} [33]. The characteristics $\nu(ClO_4^-)$ modes of the dissolved $LiClO_4$ salt represent a band around 625 cm^{-1} [28,30].

Estimation of the relative amounts of free ions and contact ion pairs in the blend hybrid SPEs is important and can be achieved by deconvoluting the FTIR spectra in the wavenumber region of 660–600 cm^{-1} that belongs to the characteristic vibrational modes of the ClO_4^- anion. Fig. S4 (SI) depicts the deconvoluted FTIR spectra of the PD(60:40)-Z blend hybrid SPEs with Gaussian-Lorentzian functions giving two peaks centered at 635 and 625 cm^{-1}. Free ClO_4^- anions (conversely, free lithium ions) contribute to the observed peak around 625 cm^{-1}, while the $Li^+ClO_4^-$ contact-ion pairs are responsible for the peak around 635 cm^{-1} [34,35]. The detailed discussion about the estimation of number of free mobile ions is presented in the SI.

3.5. Structure examination by ^{13}C and ^{29}Si CPMAS NMR

Solid-state NMR spectroscopy, especially ^{13}C and ^{29}Si CPMAS NMR, is an excellent tool to provide not only the information about the structure of the polymeric matrix, but also the backbone structure of the present hybrid system. Fig. 4A shows the ^{13}C CPMAS NMR spectra of PD(60:40)-Z blend hybrid SPEs. A sharp peak at 70 ppm is observed in all the spectra due to the carbons attached with the oxygen atoms of EO units of M-2070, ED2003 and PEGDGE [31]. Similarly, the small peak at 75 ppm can be ascribed to the carbons attached with the oxygen atoms of PO units of M-2070 and ED2003. The peak observed at 17 ppm is due to carbons from $-CH_3$ groups of PO units. The carbons from the $-CH_2$ groups of the first and second position to silicon atom in ICPTES generate peaks at 9 and 22 ppm, respectively. The appearance of the characteristics peaks from the different carbon units suggests the formation of successful blend hybrid structure.

The silica architecture in the blend hybrid system can be probed by ^{29}Si CPMAS NMR. Fig. 4B displays the ^{29}Si CPMAS NMR spectrum of PD (60:40)-32 blend hybrid SPE. As observed in the figure, the two silicon species, T^2 ($RSi(OSi)_2(OH)$, R = alkyl group) and T^3 $RSi(OSi)_3$ give rise to peaks at −59 and −67.9 ppm, respectively. The existence of T groups in the blend hybrid SPE confirms the formation of silica particles or domains within the hybrid matrix. After spectral deconvolution, it is found that the intensity of T^3 peak is 6 times higher than T^2 (T^3:T^2 = 6.4:1), indicating that the organosilane effectively condenses but still there remain a very less amount of Si–OH groups due to incomplete condensation. The dynamic behavior analysis of the blend hybrid SPEs by solid-state NMR is discussed in the SI (Fig. S5 and Fig. S6).

3.6. Mechanical properties of blend hybrid SPEs

Mechanical stability and elasticity of the SPE membranes can be evaluated from stress-strain measurements. The stress-strain curves of the PD(60:40)-Z blend hybrid SPEs are shown in Fig. 5. As observed in Fig. 5, the salt free blend hybrid membrane exhibits higher tensile stress but lower elongation in comparison to the blend hybrid SPE membranes with different salt concentrations. In the blend SPE samples, the yield-stress is decreased with the increase in salt concentrations. On the other hand, the strain percentage continuously increases with the increase in salt concentrations. The intramolecular interaction between the

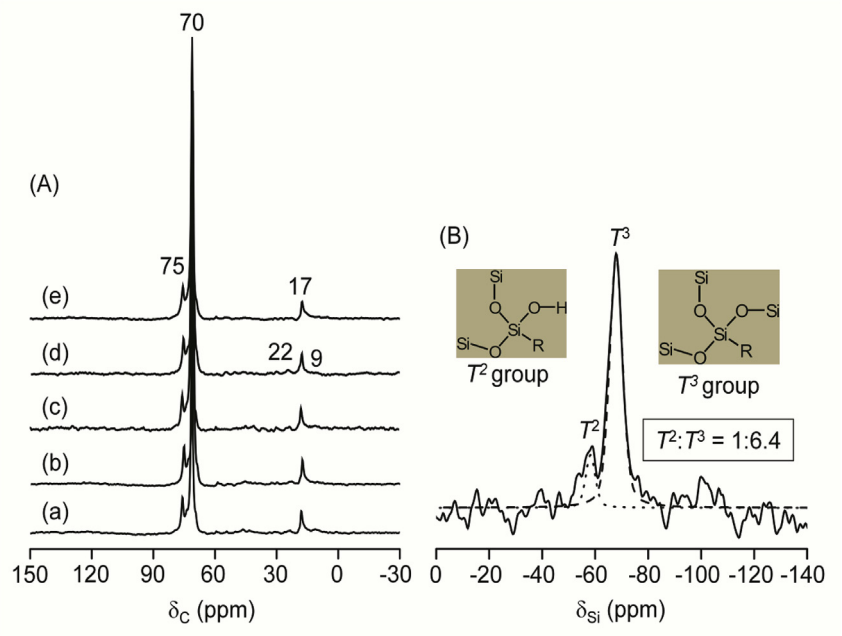

Fig. 4. (A) ^{13}C CPMAS NMR spectra of PD(60:40)-Z blend hybrid SPEs with Z = (a) 48, (b) 40, (c) 32, (d) 24, and (e) 16. (B) ^{29}Si CPMAS NMR spectrum of PD (60:40)-32 blend hybrid SPE.

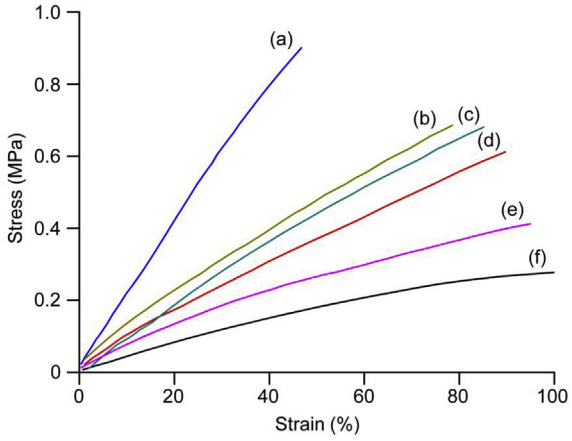

Fig. 5. Stress-strain curves of PD(60:40)-Z blend hybrid SPEs with Z = (a) ∞, (b) 48, (c) 40, (d) 32, (e) 24 and (f) 16.

polymer chains and $LiClO_4$ salt reduces the yield-stress, but makes the blend hybrid SPE membranes more elastic resulting in enhancement in the elongation of the membranes [36]. Moreover, the in-situ formed sub-micron silica particles help to improve the mechanical strength of the membranes. These silica particles are cross-linked with the polymeric units as cross-linking sites and thereby increase the degree of crosslinking as well as mechanical strength. Furthermore, the existence of the silica particles at the interface increases the stress transfer and improves the mechanical properties [37]. Overall, these blend hybrid SPE membranes are flexible and possess sufficient mechanical strength to be used as separators in LIBs.

3.7. Morphological study of blend hybrid SPEs

SEM measurements are conducted to explore whether in-situ silica particles are formed within the blend hybrid matrices to give a composite nature to the hybrid membrane. The SEM images of PD(60:40)-Z (Z = 48, 32 and 16) blend hybrid SPEs along with their silicon elemental mapping images are shown in Fig. 6. The microstructural morphology of PD(60:40)-48 shows larger sub-micron sized silica particles, which are inhomogeneously embedded in the membrane surface. When the salt concentration is increased to [O]/[Li] = 32, the morphology of the blend hybrid SPE become more homogeneous with uniformly distributed smaller silica particles as compared to the blend hybrid SPE with [O]/[Li] = 48. However, homogeneity of the blend hybrid SPE is reduced when the salt concentration is further increased to [O]/[Li] = 16. Some larger silica particles along with smaller particles are observed for PD(60:40)-16 SPE sample, possibly due to aggregation of some smaller particles. It suggests that the interactions between $LiClO_4$ and silica domains also vary with salt concentration, and hence the observed change in the size of silica particles. The silicon elemental mapping of all the above discussed SPE samples shows that silica particles are uniformly distributed on the surface of the samples with a slightly higher particle density for the PD(60:40)-32 hybrid SPE. The results suggest that good microstructural morphology with well distributed smaller sub-micron sized silica particles of the PD(60:40)-32 blend hybrid SPE membrane may be suitable for rapid charge and mass transport.

3.8. Ionic conductivity and electrochemical stability of hybrid SPEs

The temperature dependence of ionic conductivities of PD(60:40)-Z blend hybrid SPEs as a function of the lithium concentrations are depicted in Fig. 7A. As expected, the ionic conductivity constantly increases with increasing the sample temperature. A higher temperature not only stimulates the lithium ions to travel faster, but also expands the polymer network to create more free volumes. These free volumes promote enhanced activity of polymer segmental movements as well as Li^+ ions mobility by providing conductive pathways, and thus encourages ionic movements [38]. The Arrhenius plots of the conductivity data also show curved plots for the entire blend hybrid SPEs, suggesting that the ionic conductivity follows the Vogel-Tamman-Fulcher (VTF) behavior, i.e., movements of ions in the electrolytes are mainly due to the segmental movements of the polymer chains, and contribution from thermally activated ionic hopping is minimal. It is also observed that initially ionic conductivity enhances with increase in the salt concentration and has reached a maximum at [O]/[Li] = 32. Further increase in salt concentration reduces the ionic conductivity. The

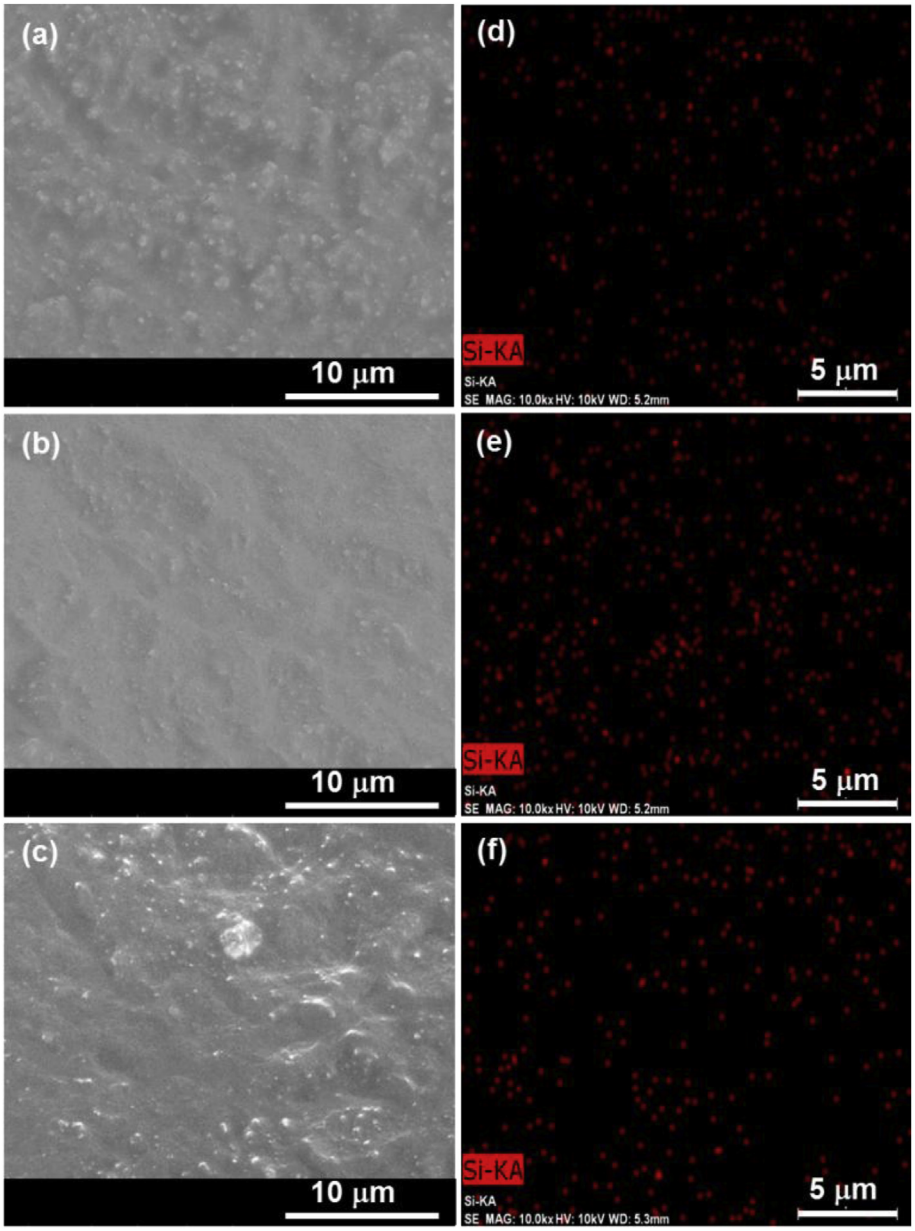

Fig. 6. SEM images and silicon elemental mapping of (a,d) PD(60:40)-48, (b,e) PD(60:40)-32 and (c,f) PD(60:40)-16 blend hybrid SPEs.

maximum ionic conductivity values of 1.1×10^{-4} and 5.8×10^{-4} S cm^{-1} are obtained for the PD(60:40)-32 hybrid SPE at 30 and 70 °C, respectively. The obtained ionic conductivity values are higher or comparable to the values reported by other researchers on similar types of hybrid electrolytes [19,39–41]. Several factors are responsible for the observed ionic conductivity (σ) and can be related to the equation,

$$\sigma(T) = \sum_i n_i q_i \mu_i \tag{4}$$

where n_i, q_i and μ_i are the number, charge and mobility of the charge carrier i. Normally, ionic conductivity enhances with increase in the number of charge carriers, which is directly related to the salt concentration. As demonstrated in the FTIR deconvoluted spectra, the number of charged ions is shown to be increased with the increase in the $LiClO_4$ concentration (Table 1). It is expected that the PD(60:40)-32 hybrid SPE sample with the highest ionic conductivity should have the largest number of charge carriers. However, both the PD(60:40)-24 and PD(60:40)-16 hybrid SPEs have more charge carriers than the PD (60:40)-32 hybrid SPE. It suggests that more number of charge carriers overcrowded the electrolytes with higher salt concentrations, and thus hampers mobility and diffusion of charged species. In addition, the formation of $Li^+ClO_4^-$ contact-ion pairs increases at higher salt concentrations because of shorter distance between cationic and anionic charges (overcrowding) enabling easier recombination. Therefore, reduced mobility and diffusion of charges, and higher number of contact-ion pairs and ion aggregates limit the effective charge carriers at higher salt concentrations. As a result, optimum effective charge carriers may be achieved for the PD(60:40)-32 hybrid SPE, leading to the maximum ionic conductivity. The glass transition temperature (T_g) also helps in the ion transport process of the blend hybrid electrolytes. As we have not detected the T_g value for the PD(60:40)-32 hybrid SPE in the measured temperature range of −50 to 100 °C, it is obvious that T_g value is below −50 °C for this sample. The lower T_g value makes the polymer chains more flexible. On the other hand, the T_g values are higher for PD(60:40)-24 (−43.6 °C) and PD(60:40)-16 (−33.7 °C). With increase in the salt concentration, the T_g values enhance and make the polymer backbone structure more rigid. The inter- and

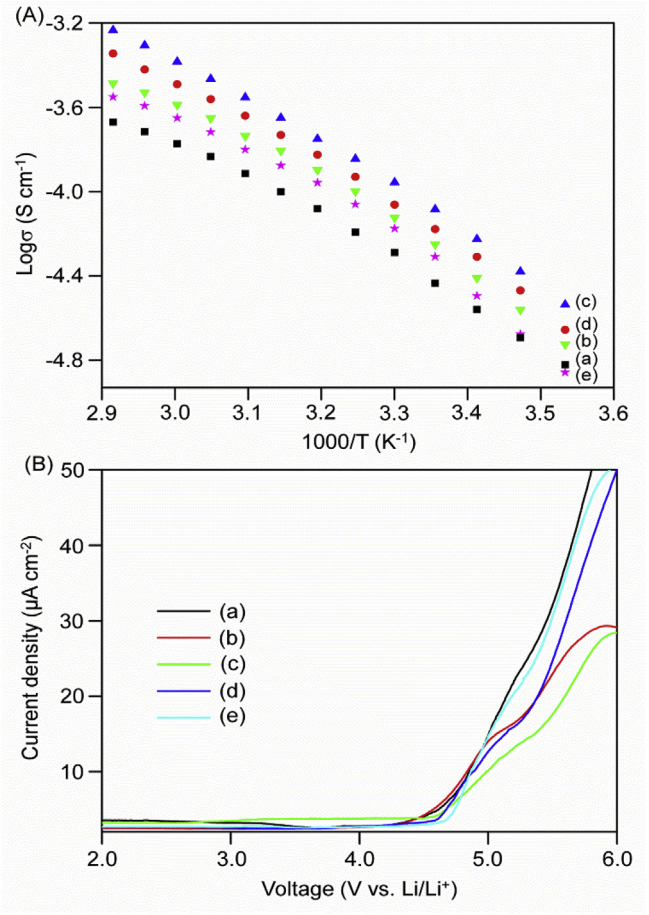

Fig. 7. Temperature dependence of ionic conductivity (A) and linear sweep voltammetry curves (B) of PD(60:40)-Z blend hybrid SPEs with Z = (a) 48, (b) 40, (c) 32, (d) 24 and (e) 16.

intramolecular coordination of ether dipoles with the charge carriers may act as cross-linking points, which in turn enhances the T_g of the blend hybrid SPEs. The higher T_g values reduce the free volume and the polymer segmental motion, and thereby decrease the ionic conductivity. Therefore, all the above mentioned factors play a role in making the PD(60:40)-32 sample to be the best blend hybrid SPE.

Another important observation is that the blend hybrid SPEs behave as composite SPEs due to the formation of in-situ sub-micron sized silica particles within the SPE framework owing to the use of ICPTES. As observed in the SEM analysis and elemental mapping of SPEs, the in-situ formed sub-micron silica particles are well dispersed throughout the blend hybrid SPEs, and specifically the PD(60:40)-32 sample shows a higher concentration of silica particles than the other blend hybrid SPEs. These silica particles reduce the polymer-cation interactions, enhance the amorphous phase and finally increase the ionic conductivity [42]. In addition, polymer-silica interaction generates a highly conducting interface layer through which ions can move rapidly and enhance the ionic conductivity [43]. These interface layers or so called grain boundaries are the sites of high defect concentration regions, which act as channels for the rapid movement of ions and lead to enhancement in ionic conductivity [44]. From SEM analysis, it is also observed that the PD(60:40)-32 hybrid SPE possesses smaller but a larger number of silica particles than other samples. Therefore, it suggests that these smaller silica particles may generate more grain boundaries due to increase in the surface area and larger numbers of particles, and thus contribute in the rapid movements of ions leading to enhancement in ionic conductivity. Hence, the in-situ formed silica particles play a critical role in delivering the maximum ionic conductivity for the PD(60:40)-32 hybrid SPE among the blend hybrid SPEs investigated. In addition, ionic conductivity may be influenced by the Lewis acid/base reactions among EO/PO segments, silica particles and anions of the lithium salt [45,46]. The Lewis acid –OH groups on the surface of silica particles (confirmed from ^{29}Si CPMAS NMR) interact with the ether oxygen atoms of EO/PO segments and ClO_4^- anions of the $LiClO_4$ salt. This leads to an increase in amorphous phase by restricting the PEO/PPO chains reorganization and less mobility of the ClO_4^- anions, which in turn helps in the formation of Li^+-ion conducting pathways on the surfaces of silica particles. The –OH groups can reduce the movement of ClO_4^- and ionic coupling by their interactions with the ClO_4^- anions. As a result, they facilitate more free lithium ions leading to increase in the ionic conductivity [46]. Therefore, the present blend hybrid SPEs exhibit relatively high ionic conductivity values of the order of 10^{-4} S cm^{-1} at room temperature.

The electrochemical stability window of the PD(60:40)-Z blend hybrid SPEs is measured to explore the voltage limit of the membranes which they can withstand when use in a battery. Fig. 7B shows the linear sweep voltammetry curves of the blend hybrid SPEs in the voltage range of 0–6 V. A very low background current observes in the potential region of 2–4.5/4.7 V for the entire blend hybrid SPEs due to the changes in the surface of stainless steel electrode [47]. After crossing the 4.5/4.7 V voltage limit, the current starts to increase rapidly due to decomposition of blend hybrid SPEs. A small increase in the electrochemical stability window is detected when the salt concentration increases. For example, the electrochemical stability window of 4.5 V is observed for [O]/[Li] = 48 and 40, about 4.6 V for [O]/[Li] = 32 and 24, and around 4.7 V for [O]/[Li] = 16. It suggests that anion oxidation may decompose the electrolytes and lower the electrochemical stability window with the decrease in salt concentrations. As revealed by FTIR study, higher percentages of free anions are available at lower salt concentrations than at higher salt concentrations, which are oxidized easily to lower the stability windows for the PD (60:40)-48 and PD(60:40)-40 blend hybrid SPEs. The dissociations of anions are less at higher salt concentrations, which helps to extend the stability window to 4.7 V for the PD(60:40)-16 SPE sample. In general, the electrochemical stability windows of 4.5–4.7 V for the blend hybrid SPEs are suitable for their possible use in lithium-ion batteries.

3.9. Transformation of SPEs to PPEs

Although a relatively high ionic conductivity of the order of 10^{-4} S cm^{-1} is achieved for the blend hybrid SPEs, it is still not sufficient to get a good cycle performance in lithium-ion batteries at room temperature when used as an electrolyte. Therefore, the blend hybrid membrane without the dopant salt, i.e., PD(60:40)-∞, is swelled in different organic electrolyte solvents to make the hybrid plasticized polymer electrolytes (denoted as PPEs) with enhanced ionic conductivity for practical applications. Some electrochemical characterizations are carried out on PPEs to evaluate their performances in lithium-ion batteries.

3.10. Swelling behavior, ionic conductivity and electrochemical stability of blend hybrid PPEs

The “salt free” blend hybrid membrane is dipped in organic electrolyte solvents of 1 M LiOTf in EC/PC (1:1, v/v), 1 M $LiPF_6$ in EC/DEC (1:1, v/v) and 1 M LiTFSI in EC/PC (1:1, v/v) to determine the swelling ratio (SR) of the membrane by following the equation,

$$SR(\%) = \frac{W - W_0}{W_0} \times 100 \quad (5)$$

where W_0 and W represent the weights of the membrane before and after dipping in solvents, respectively. The swelling behavior of the blend hybrid membrane in different electrolyte solvents is depicted in Fig. S7 (SI). As seen in Fig. S7, the membrane swollen with 1 M LiOTf in

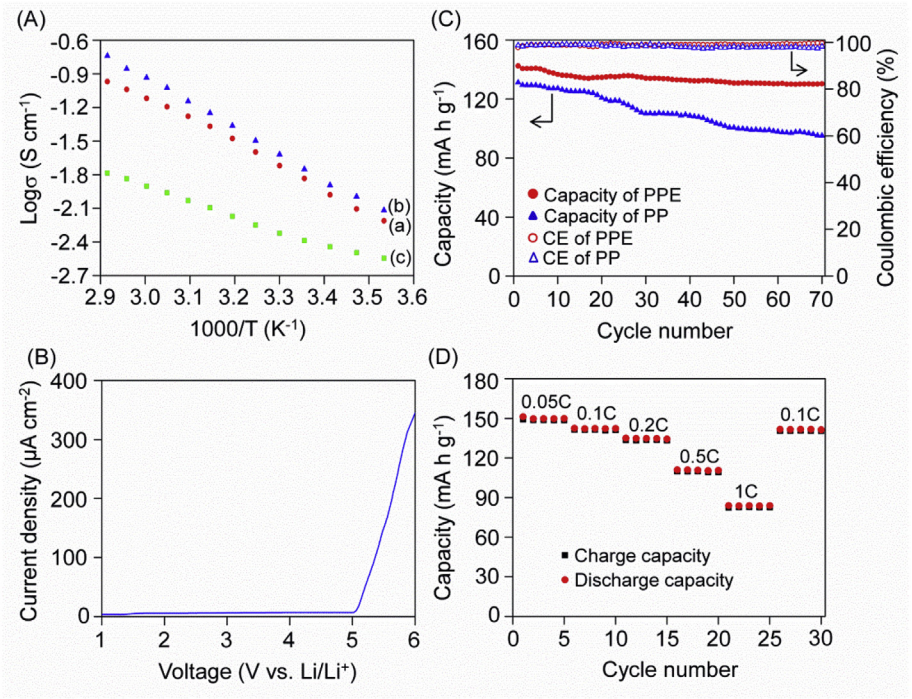

Fig. 8. (A) Temperature dependence ionic conductivity of PD(60:40)-∞ plasticized blend hybrid electrolytes in (a) 1 M LiOTf in EC/PC, (b) 1 M $LiPF_6$ in EC/DEC, (c) 1 M LiTFSI in EC/PC. (B) Linear sweep voltammetry curve of PD(60:40)-∞ PPE membrane in 1 M $LiPF_6$ in EC/DEC. (C) Discharge capacities and coulombic efficiencies of cells prepared with PD(60:40)-∞ hybrid PPE and standard polypropylene membranes in 1 M $LiPF_6$ in EC/DEC. (D) Rate performance of the cell prepared with PD (60:40)-∞ hybrid PPE membrane in 1 M $LiPF_6$ in EC/DEC.

EC/PC (1:1, v/v) delivers the maximum swelling ratio of 618% within 30 min of dipping time. However, the swelling ratio starts to decrease due to the extrusion of the electrolyte solvent from the membrane. On the other hand, the membranes with 1 M $LiPF_6$ in EC/DEC (1:1, v/v) and 1 M LiTFSI in EC/PC (1:1, v/v) show the maximum swelling percentages of 553% and 534%, respectively, after 60 min only. The higher swelling percentages suggest good porosity of hybrid PPEs. The difference in swelling ratios by different electrolyte solvents also suggests the influence induced by the viscosity and size of the molecules in the solvents. It is also observed that swelling percentage reaches saturation state in the membrane with 1 M $LiPF_6$ in EC/DEC after 60 min and more stable in comparison to the membranes with other two electrolyte solvents with retaining the electrolyte solvent in the pores more efficiently for longer time. However, a prolonged dipping time may make the membranes brittle. Therefore, a dipping time of 30 min is selected for the membranes to measure ionic conductivity and to test the lithium-ion battery without compromising mechanical properties.

The temperature dependent ionic conductivities of the PD(60:40)-∞ (i.e., salt free) membrane in three different electrolyte solvents are measured and displayed in Fig. 8A. The results show the Arrhenius-like behavior of ionic conductivity enhancement with the increase in temperature and suggest that ions are decoupled from the segmental chain movements and thermally activated ionic hopping plays the major role in ions transport. The plasticized blend hybrid membranes with different electrolyte solvents exhibit outstanding ionic conductivity values of 2.4×10^{-2} S cm^{-1} (1 M $LiPF_6$ in EC/DEC), 1.9×10^{-2} S cm^{-1} (1 M LiOTf in EC/PC) and 4×10^{-3} S cm^{-1} (1 M LiTFSI in EC/PC) at 30 °C. At 70 °C, the blend hybrid membrane with 1 M $LiPF_6$ in EC/DEC delivers maximum ionic conductivity of 1.8×10^{-1} S cm^{-1}. These values are remarkably higher than the previously reported literature [48–50]. Achievement of such a high ionic conductivity is mainly attributed to the large electrolyte uptake of the membrane. Besides, dielectric constant and viscosity of the solvents use to play an important role in achieving different ionic conductivity values with different electrolyte solvents. It is suggested that the electrolyte solvents are initially absorbed inside the pores of the membrane, and slowly started to infiltrate into the polymer chains and finally swelled the amorphous domains [51,52]. Since the carbonyl solvents are preferable for coordination with Li^+ ions, the blend hybrid membrane can retain a large amount of solvents in the pores for coordination. As a result, the free lithium ions can move rapidly through these pores and swollen amorphous regions, and lead to such high ionic conductivity values.

The electrochemical stability of the PD(60:40)-∞ blend hybrid PPE membrane is tested with the electrolyte solvent of 1 M $LiPF_6$ in EC/DEC (1:1, v/v), which achieves the highest ionic conductivity value among the electrolyte solvents used. The LSV curve (Fig. 8B) of the hybrid PPE membrane shows that a very low background current flows in the cell between the potentials of 1 and 5 V. The current has started to increase rapidly when it crossed 5 V due to the decomposition of the hybrid PPE membrane, indicating the stability limit of the membrane. The obtained electrochemical stability window of 5 V is good enough to use the blend hybrid PPE membrane both as the separator and the electrolyte in most of the lithium-ion batteries. It is quite possible that the obtained electrochemical stability window may influence by the Si–OH groups present in the hybrid membrane. The Si–OH groups may form a thin layer on the lithium electrode's surface and prevent the hybrid PPE membrane from decomposition and keep it electrochemically stable up to 5 V.

3.11. Cycle and rate performance of the hybrid PPE

The best ion conductive PPE membrane based on PD(60:40)-∞ with 1 M $LiPF_6$ in EC/DEC is used to measure the cycle and rate performance of the cell by using lithium as anode and $LiFePO_4$ as cathode in the voltage range of 2.6–4.2 V. The cycle performance is also compared with the polypropylene (PP) membrane commonly used in LIBs as separator. Fig. 8C displays the discharge capacity and coulombic efficiency values of the hybrid PPE and PP membranes at a current rate of 0.1C. The initial discharge capacities are 142.5 and 131.2 mA h g^{-1} for hybrid PPE and PP membranes, respectively, which decrease to 130.4 and 95.2 mA h g^{-1} after 70 cycles. The decrease in capacity is ascribed to the formation of solid electrolyte interface (SEI) layer at the lithium/electrolyte junction [53]. The decomposition of electrolyte in contact with lithium electrode forms a passivation film on the surface of the electrode, which prohibits the usual charge and mass transport and consumes part of the anode capacity leading to irreversible capacity loss. However, this passivation layer also protects the hybrid PPE membrane from further reduction by the lithium electrode, and thus

assists in delivering stable capacity. It is observed that after continuous reduction in capacity up to 35 cycles, the hybrid PPE electrolyte delivers a stable capacity of 130 mA h g^{-1} between 35 and 70 cycles, whereas the capacity reduces continuously in the case of PP membrane due to the formation of unstable and non-uniform SEI layer. After 70 cycles, the hybrid PPE membrane retains 92% of initial capacity compared to 72% of standard PP membrane. Thus, the capacity of the hybrid PPE membrane is 1.4 times higher than the PP membrane at 70th cycle.

For the hybrid PPE membrane, the first cycle coulombic efficiency (CE) value is 97.8% which is gradually increased to 99% in the 8th cycle and from 37 to 70 cycles it maintains the CE values of 99–99.7%. On the other hand, the PP membrane exhibits an initial CE value of 98.7% and is gradually enhanced to 99% in the 7th cycle. However, its CE value starts to drop from 20th cycle onwards and displays values between 97.6% and 98.2% up to 70th cycle. In comparison to the case of the PP membrane, the higher CE values of the hybrid PPE membrane reveal better reversible charge transfer reactions that occur at the stable electrode/electrolyte interface.

The rate capability data of the hybrid PPE membrane is presented in Fig. 8D. As seen in Fig. 8D, the hybrid PPE based cell delivers a discharge capacity of 152 mA h g^{-1} at 0.05C, which is closer to the theoretical capacity of $LiFePO_4$ (165 mA h g^{-1}). With rise in the current rates from 0.05C to 0.1C, 0.2C, 0.5C and 1C, the cell delivers almost stable discharge capacities of 142, 135, 111 and 84 mA h g^{-1}, respectively. When the current rate is again back to 0.1C after 25 cycles, the cell still delivers the nearly same discharge capacity of 141 mA h g^{-1} as the previous one. Therefore, the cell can retain almost 99.3% capacity after 25 cycles at a current rate of 0.1C. The results suggest the robustness and good compatibility of the hybrid PPE membrane and electrodes even after undergoing a high rate cycling. The good electrolyte/electrode interfacial contact may also help in improving the reaction kinetics and in achieving stable rate capacities.

4. Conclusions

A new blend hybrid SPE has been successfully synthesized by blending the precursors from amine ended block co-polymers of ethylene oxide/propylene oxide, poly(ethylene glycol) diglycidyl ether and (3-isocyanatopropyl)triethoxysilane and its performance is evaluated in a lithium-ion battery. Morphological, thermal and structural investigations confirm the successful synthesis of the blend hybrid with mechanical and thermal integrity along with sufficient flexibility. The solid blend hybrid SPEs possess the maximum ionic conductivities of 1.1×10^{-4} S cm^{-1} at 30 °C and 5.8×10^{-4} S cm^{-1} at 70 °C with an electrochemical stability window of 4.5–4.7 V. After plasticization, the hybrid PPE membrane achieves outstanding ionic conductivity values of 2.4×10^{-2} and 1.8×10^{-1} S cm^{-1} at 30 and 70 °C, respectively, with an electrochemical stability window extended to 5 V. The cycle performances of the lithium-ion batteries with the hybrid PPE membrane as separator are compared with the standard polypropylene membrane, and found to be 1.4 times higher than the latter. The test cell delivers an initial discharge capacity value of 142.5 mA h g^{-1} with capacity retention of 92% and coulombic efficiency of over 99% after 70 cycles at a current rate of 0.1C. The discharge capacity can be enhanced to 152 mA h g^{-1} at a current rate of 0.05C. With these intriguing properties, the present blend hybrid electrolyte system demonstrates its potential to be used in lithium-ion batteries.

Acknowledgements

The financial support for this work from the Ministry of Science and Technology of Taiwan (Grant number: MOST 105-2119-M-008-012) is gratefully acknowledged.

Appendix A. Supplementary data

Supplementary data related to this article can be found at http://dx.doi.org/10.1016/j.jpowsour.2018.04.028.

References

[1] N. Nitta, F. Wu, J.T. Lee, G. Yushin, Li-ion battery materials: present and future, Mater. Today 18 (2015) 252–264.
[2] G.E. Blomgren, The development and future of lithium ion batteries, J. Electrochem. Soc. 164 (2017) A5019–A5025.
[3] K. Xu, Nonaqueous liquid electrolytes for lithium-based rechargeable batteries, Chem. Rev. 104 (2004) 4303–4418.
[4] J.B. Goodenough, K.-S. Park, The Li-ion rechargeable battery: a perspective, J. Am. Chem. Soc. 135 (2013) 1167–1176.
[5] P. Bron, S. Johansson, K. Zick, J.S. auf der Gunne, S. Dehnen, B. Roling, $Li_{10}SnP_2S_{12}$: an affordable lithium superionic conductor, J. Am. Chem. Soc. 135 (2013) 15694–15697.
[6] J. Zhang, J. Zhao, L. Yue, Q. Wang, J. Chai, Z. Liu, X. Zhou, H. Li, Y. Guo, G. Cui, Safety-reinforced poly(propylene carbonate)-based all-solid-state polymer electrolyte for ambient-temperature solid polymer lithium batteries, Adv. Energy Mat. 5 (2015) 1501082.
[7] L. Long, S. Wang, M. Xiao, Y. Meng, Polymer electrolytes for lithium polymer batteries, J. Mater. Chem. A 4 (2016) 10038–10069.
[8] D.E. Fenton, J.M. Parker, P.V. Wright, Complexes of alkali metal ions with poly (ethylene oxide), Polymer 14 (1973) 589.
[9] M.B. Armand, J.M. Chabagno, P. Vashisha, J.N. Mundy, G.K. Shenoy (Eds.), M. Duclot in Fast Ion Transport in Solids, 1979 North Holland, Amsterdam.
[10] D. He, D.W. Kim, J.S. Park, S.Y. Cho, Y. Kang, Electrochemical properties of semi-interpenetrating polymer network solid polymer electrolytes based on multi-armed oligo(ethyleneoxy) phosphate, J. Power Sources 244 (2013) 170–176.
[11] C.A. Nguyen, S. Xiong, J. Ma, X. Lu, P.S. Lee, High ionic conductivity P(VDF-TrFE)/PEO blended polymer electrolytes for solid electrochromic devices, Phys. Chem. Chem. Phys. 13 (2011) 13319–13326.
[12] X. Zuo, X.-M. Liu, F. Cai, H. Yang, X.-D. Shen, G. Liu, A novel all-solid electrolyte based on a co-polymer of poly-(methoxy/hexadecal-poly(ethylene glycol) methacrylate) for lithium-ion cell, J. Mater. Chem. 22 (2012) 22265–22271.
[13] J. Nunes-Pereira, C.M. Costa, S. Lanceros-Méndez, Polymer composites and blends for battery separators: state of the art, challenges and future trends, J. Power Sources 281 (2015) 378–398.
[14] L. Yue, J. Ma, J. Zhang, J. Zhao, S. Dong, Z. Liu, G. Cui, L. Chen, All solid-state polymer electrolytes for high-performance lithium ion batteries, Energy Storage Mat. 5 (2016) 139–164.
[15] J. Ji, J. Keen, W.-H. Zhong, Simultaneous improvement in ionic conductivity and mechanical properties of multi-functional block-copolymer modified solid polymer electrolytes for lithium ion batteries, J. Power Sources 196 (2011) 10163–10168.
[16] A.I. Gopalan, P. Santhosh, K.M. Manesh, J.H. Nho, S.H. Kim, C.-G. Hwang, K.-P. Lee, Development of electrospun PVdF–PAN membrane-based polymer electrolytes for lithium batteries, J. Membr. Sci. 325 (2008) 683–690.
[17] P. Judeinstein, J. Titman, M. Stamm, H. Schmidt, Investigation of ion-conducting ormolytes: structure-property relationships, Chem. Mater. 6 (1994) 127–134.
[18] D. Saikia, Y.-C. Pan, C.-G. Wu, J. Fang, L.-D. Tsai, H.-M. Kao, Synthesis and characterization of a highly conductive organic–inorganic hybrid polymer electrolyte based on amine terminated triblock polyethers and its application in electrochromic devices, J. Mater. Chem. C 2 (2014) 331–343.
[19] J. Shim, D.-G. Kim, J.H. Lee, J.H. Baik, J.-C. Lee, Synthesis and properties of organic/inorganic hybrid branched-graft copolymers and their application to solid-state electrolytes for high-temperature lithium-ion batteries, Polym. Chem. 5 (2014) 3432–3442.
[20] P. Carol, P. Ramakrishnan, B. John, G. Cheruvally, Preparation and characterization of electrospun poly(acrylonitrile) fibrous membrane based gel polymer electrolytes for lithium-ion batteries, J. Power Sources 196 (2011) 10156–10162.
[21] S.-H. Wang, S.-S. Hou, P.-L. Kuo, H.-S. Teng, Poly(ethylene oxide)-co-poly(propylene oxide)-based gel electrolyte with high ionic conductivity and mechanical integrity for lithium-ion batteries, ACS Appl. Mater. Interfaces 5 (2013) 8477–8485.
[22] D. Saikia, H.-Y. Wu, Y.-C. Pan, C.-P. Lin, K.-P. Huang, K.-N. Chen, G.T.K. Fey, H.-M. Kao, Highly conductive and electrochemically stable plasticized blend polymer electrolytes based on PVdF-HFP and triblock copolymer PPG-PEG-PPG diamine for Li-ion batteries, J. Power Sources 196 (2011) 2826–2834.
[23] J. Xi, X. Qiu, X. Ma, M. Cui, J. Yang, X. Tang, W. Zhu, L. Chen, Composite polymer electrolyte doped with mesoporous silica SBA-15 for lithium polymer battery, Solid State Ionics 176 (2005) 1249–1260.
[24] W.A. Henderson, Crystallization kinetics of glyme − LiX and PEO − LiX polymer electrolytes, Macromolecules 40 (2007) 4963–4971.
[25] J.F. Le Nest, A. Gandini, C. Schoenenberger, Elastomeric polymer electrolytes based on crosslinked polyethers: the state of the art, Trends Polym. Sci. 2 (1994) 432–437.
[26] M.M. Coleman, K.H. Lee, D.J. Skrovanek, P.C. Painter, Hydrogen bonding in polymers. 4. Infrared temperature studies of a simple polyurethane, Macromolecules 19 (1986) 2149–2157.
[27] L.S. Teo, C.Y. Chen, J.F. Kuo, Fourier transform infrared spectroscopy study on effects of temperature on hydrogen bonding in amine-containing polyurethanes and poly(urethane-urea)s, Macromolecules 30 (1997) 1793–1799.
[28] D.L. Pavia, G.M. Lampman, G.S. Kriz, Introduction to Spectroscopy, Harcourt College Publication, USA, 2001, pp. 15–84.

[29] T. Miyazawa, T. Shimanouchi, S.-I. Mizushima, Characteristic infrared bands of monosubstituted amides, J. Chem. Phys. 24 (1956) 408–418.
[30] P. Patnaik, Dean's Analytical Chemistry Handbook, second ed., McGraw-Hill, New York, 2004, pp. 7.1–7.43.
[31] H.-M. Kao, T.T. Hung, G.T.K. Fey, Multinuclear solid-state NMR characterization, ion dissociation, dynamic properties of lithium-doped organic–inorganic hybrid electrolytes based on ureasils, Macromolecules 40 (2007) 8673–8683.
[32] A. Kioul, L. Mascia, Compatibility of polyimide-silicate ceramers induced by alkoxysilane coupling agents, J. Non-Cryst. Solids 175 (1994) 169–186.
[33] M.M. Silva, V. de Zea Bermudez, L.D. Carlos, A.P.P. de Almeida, M.J. Smith, Sol-gel processing and structural study of europium-doped hybrid materials, J. Mater. Chem. 9 (1999) 1735–1740.
[34] M. Salomon, M. Xu, E.M. Eyring, S. Petrucci, Molecular structure and dynamics of $LiClO_4$-polyethylene oxide-400 (dimethyl ether and diglycol systems) at 25°C, J. Phys. Chem. 98 (1994) 8234–8244.
[35] H.-W. Chen, C.-Y. Chiu, H.-D. Wu, I.-W. Shen, F.-C. Chang, Solid-state electrolyte nanocomposites based on poly(ethylene oxide), poly(oxypropylene) diamine, mineral clay and lithium perchlorate, Polymer 43 (2002) 5011–5016.
[36] M.M.E. Jacob, A.K. Arof, Mechanical studies on poly(vinylidene fluoride) based polymer electrolytes, Polym. Eng. Sci. 40 (2000) 972–978.
[37] S. Ramesh, T. Winie, A.K. Arof, Investigation of mechanical properties of polyvinyl chloride-polyethylene oxide (PVC–PEO) based polymer electrolytes for lithium polymer cells, Eur. Polym. J. 43 (2007) 1963–1968.
[38] M. Ulaganathan, C.M. Mathew, S. Rajendran, Highly porous lithium-ion conducting solvent-free poly(vinylidene fluoride-co-hexafluoropropylene)/poly(ethyl methacrylate) based polymer blend electrolytes for Li battery applications, Electrochim. Acta 93 (2013) 230–235.
[39] P.C. Barbosa, M.M. Silva, M.J. Smith, A. Gonçalves, E. Fortunato, S.C. Nunes, V. de Zea Bermudez, Di-ureasil xerogels containing lithium bis(trifluoromethanesulfonyl) imide for application in solid-state electrochromic devices, Electrochim. Acta. 54 (2009) 1002–1009.
[40] S.C. Nunes, V. de Zea Bermudez, D. Ostrovskii, M.M. Silva, S. Barros, M.J. Smith, L.D. Carlos, J. Rocha, E. Morales, Diurea cross-linked poly(oxyethylene)/siloxane ormolytes for lithium batteries, J. Electrochem. Soc. 152 (2005) A429–A438.
[41] D. Saikia, H.-Y. Wu, C.-P. Lin, Y.-C. Pan, J. Fang, L.-D. Tsai, G.T.K. Fey, H.-M. Kao, New highly conductive organic-inorganic hybrid electrolytes based on star-branched silica based architectures, Polymer 53 (2012) 6008–6020.
[42] Y. Dai, S. Greenbaum, D. Golodnitsky, G. Ardel, E. Strauss, E. Peled, Y. Rosenberg, Lithium-7 NMR studies of concentrated LiI/PEO-based solid electrolytes, Solid State Ionics 106 (1998) 25–32.
[43] C.W. Nan, D.M. Smith, A.c. electrical properties of composite solid electrolytes, Mater. Sci. Eng. B 10 (1991) 99–106.
[44] J. Maier, Ionic conduction in space charge regions, Prog. Solid State Chem. 23 (1995) 171–263.
[45] W. Wieczorek, J.R. Stevens, Z. Florjańczyk, Composite polyether based solid electrolytes. the Lewis acid-base approach, Solid State Ionics 85 (1996) 67–72.
[46] F. Croce, L. Persi, B. Scrosati, F. Serraino-Fiory, E. Plichta, M.A. Hendrickson, Role of the ceramic fillers in enhancing the transport properties of composite polymer electrolytes, Electrochim. Acta. 46 (2001) 2457–2461.
[47] A.C. Bloise, J.P. Donoso, C.J. Magon, A.V. Rosario, E.C. Pereira, NMR and conductivity study of PEO-based composite polymer electrolytes, Electrochim. Acta. 48 (2003) 2239–2246.
[48] R. Tan, R. Gao, Y. Zhao, M. Zhang, J. Xu, J. Yang, F. Pan, Novel organic–inorganic hybrid electrolyte to enable $LiFePO_4$ quasi-solid-state Li-ion batteries performed highly around room temperature, ACS Appl. Mater. Interfaces 8 (2016) 31273–31280.
[49] Y. Wang, J. Qiu, J. Peng, J. Li, M. Zhai, One-step radiation synthesis of gel polymer electrolytes with high ionic conductivity for lithium-ion batteries, J. Mater. Chem. A 5 (2017) 12393–12399.
[50] W. Li, Y. Pang, J. Liu, G. Liu, Y. Wang, Y. Xia, A PEO-based gel polymer electrolyte for lithium ion batteries, RSC Adv. 7 (2017) 23494–23501.
[51] Y. Saito, H. Kataoka, E. Quartarone, P. Mustarelli, Carrier migration mechanism of physically cross-linked polymer gel electrolytes based on PVDF membranes, J. Phys. Chem. B 106 (2002) 7200–7204.
[52] Z. Li, G. Su, X. Wang, D. Gao, Micro-porous P(VDF-HFP)-based polymer electrolyte filled with Al_2O_3 nanoparticles, Solid State Ionics 176 (2005) 1903–1908.
[53] H.-H. Kuo, W.-C. Chen, T.-C. Wen, A. Gopalan, A novel composite gel polymer electrolyte for rechargeable lithium batteries, J. Power Sources 110 (2002) 27–33.